Robot vs chamber calibration-derived antenna PCC models differences and their impact on GNSS positioning: LEIAR25 case study

G. Krzan, K. Dawidowicz, P. Wielgosz
Institute of Geodesy, University of Warmia and Mazury in Olsztyn, Poland
ul. Oczapowskiego 1, 10-720 Olsztyn
grzegorz.krzan@uwm.edu.pl

EUREF 2019 Symposium, Tallin 21-24 May 2019

Introduction

In recent years, the Global Navigation Satellite Systems (GNSS) have been intensively modernized resulting in the introduction of new carrier frequencies in Global Positioning System (GPS) and Global Navigation Satellite System (GLONASS) and development of new satellite systems: Galileo and BeiDou Navigation Satellite System (BDS). For this reason, the results of the absolute field antenna calibrations, performed so far for only two legacy carrier frequencies of the GPS and GLONASS systems, seem to be insufficient. Hence, all antennas which are used in precise surveying and geodetic applications will require a re-calibration of their phase center variations (PCV) for the new signals, to ensure the highest measurement accuracy. Currently, two absolute methods are used to calibrate GNSS antennas: field calibration using robot and calibration in an anechoic chamber. Unfortunately, differences in these methodologies also result in disparity in the obtained antenna phase center corrections (PCC). We analyze the differences between individual PCC obtained with the two abovementioned calibration methods. In addition, the influence of PCC differences on GNSS-derived position time series for 19 EUREF Permanent GNSS Network (EPN) stations was also assessed. The obtained results show that the calibration method has a visible impact on PCC models. PCC differences determined for ionospheric-free combination may reach up to over 20 mm, and are transferred to the position domain. Further tests show that height component differences reach up to over 10 mm for some stations, depending on the type of the used PCC model.

Data and Method

GNSS data from 19 EPN stations (Table 1) covering the whole year of 2017 were used for the analyses in the positioning domain. Individual antenna calibrations in the anechoic chamber were performed by the Institute of Geodesy and Geoinformation (IGG), University of Bonn. Calibrations using the absolute field method were carried out by Geo++ company (Garbsen, Germany). The precise point positioning (PPP) technique, was utilized in the study to obtain precise position of the analyzed stations. For all calculations we used the NAvigation Package for Earth Observation Satellites (NAPEOS) software. Detailed parameters of the processing are presented in the Table 2.

Moreover we compared the results of calibration carried out in the anechoic chamber and using the absolute field calibration method for selected examples of tested antennas to analyse the differences in PCC models (Fig 1 and 2). In order to achieve a common datum, the results of chamber-derived PCV were shifted to PCV(α, 0) = 0, as it is adopted in robot calibrations. This was done by adding to all chamber-derived PCV a constant shift δ equal to:

$$\delta=-PCV(a,0)$$

Next step was reducing PCC values obtained during calibration in the anechoic chamber to the PCO obtained as a result of absolute field calibration, which can be done using general formula:

$$PCC(\alpha,z)=s^T\, PCO_R+(PCV_R\,(\alpha,z)+s^T\,(PCO_C-PCO_R\,))$$

where PCC – reduced chamber-derived PCC to PCO obtained as a result of absolute field calibration, PCO_R – robot-derived PCO, PCV_C – chamber-derived PCV, PCO_C – chamber-derived PCO.

The resulting robot and chamber-derived PCV were compared by forming difference patterns (dPCC) and then dPCC for L1, L2 as well as for ionospheric-free combination (IF) were calculated for GPS, GLONASS and Galileo signals.

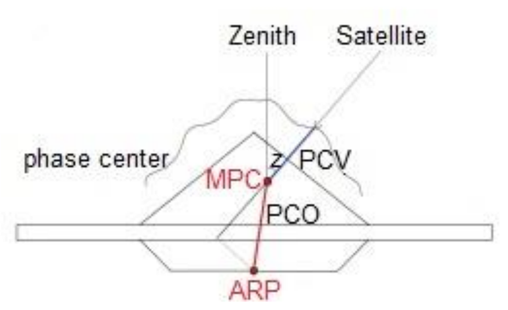

Fig 1. Main receiver antenna points and their spatial relations

Tab. 1. Hardware characteristics of the test stations

No.	Station	Network	Station hardware	
			Antenna type	Receiver type
1	AUBG	EPN	**LEIAR25.R4 LEIT**	LEICA GR25
2	BORJ	EPN	**LEIAR25.R3 LEIT**	JAVAD TRE_3 DELTA
3	DIEP	EPN	**LEIAR25.R4 LEIT**	LEICA GR25
4	DILL	EPN	**LEIAR25.R4 LEIT**	LEICA GR25
5	DOUR	EPN	**LEIAR25.R3 NONE**	SEPT POLARX4
6	EUSK	EPN	**LEIAR25.R4 LEIT**	LEICA GR25
7	GELL	EPN	**LEIAR25.R4 LEIT**	LEICA GR25
8	GOR2	EPN	**LEIAR25.R4 LEIT**	LEICA GR25
9	HEL2	EPN	**LEIAR25.R3 LEIT**	LEICA GR25
10	HELG	EPN	**LEIAR25.R4 LEIT**	JAVAD TRE_G3TH DELTA
11	HOFJ	EPN	**LEIAR25.R4 LEIT**	LEICA GR25
12	ISTA	EPN	**LEIAR25.R4 LEIT**	LEICA GR25
13	KARL	EPN	**LEIAR25.R4 LEIT**	JAVAD TRE_3 DELTA
14	LDB2	EPN	**LEIAR25.R4 LEIT**	LEICA GR25
15	LEIJ	EPN	**LEIAR25.R3 LEIT**	JAVAD TRE_G3TH DELTA
16	RANT	EPN	**LEIAR25.R4 LEIT**	JAVAD TRE_G3TH DELTA
17	SAS2	EPN	**LEIAR25.R4 LEIT**	JAVAD TRE_G3TH DELTA
18	WARN	EPN	**LEIAR25.R3 LEIT**	JAVAD TRE_G3TH DELTA
19	WRLG	EPN	**LEIAR25.R3 LEIT**	LEICA GR25

Tab. 2. Detailed parameters of the test PPP solution

Basic observables	Undifferenced carrier phases & pseudoranges;
Orbit & clock products	ESA precise final orbit and clock (30 s) products;
Ionospheric delay	1st order effect: accounted for dual frequency ionosphere-free linear combination; 2nd order effect: no corrections applied;
Tropospheric delay	Zenith dry delay computed using the Saastamoinen model with pressure and temperature from the GPT model; the resulting zenith delay is mapped using the dry GMF mapping function; wet delay estimated using the wet GMF mapping function;
Ocean loadings	Computed for FES2004 model using ONSALA ocean loading service;
Tidal displacement	In accordance with IERS2010 (Petit and Luzum 2010);
Satellite clock correction	2nd order relativistic correction for non-zero orbit ellipticity (-2*R*V / c) applied;
Observation weighting	Carrier phase: 10 mm sigma (for zenith); Pseudorange: 1 m sigma (for zenith); Sigmas increase with increasing zenith angle using the function (1 / cos(z));
Others	GPS , GLONASS, Galileo and GNSS solutions Observation sampling rate: 5 minutes; Elevation angle cut-off 5°; 365 daily sessions Results in ETRF2014 (Fig. 4 and Tab. 3) compared to C2010 EPN cumulative solution

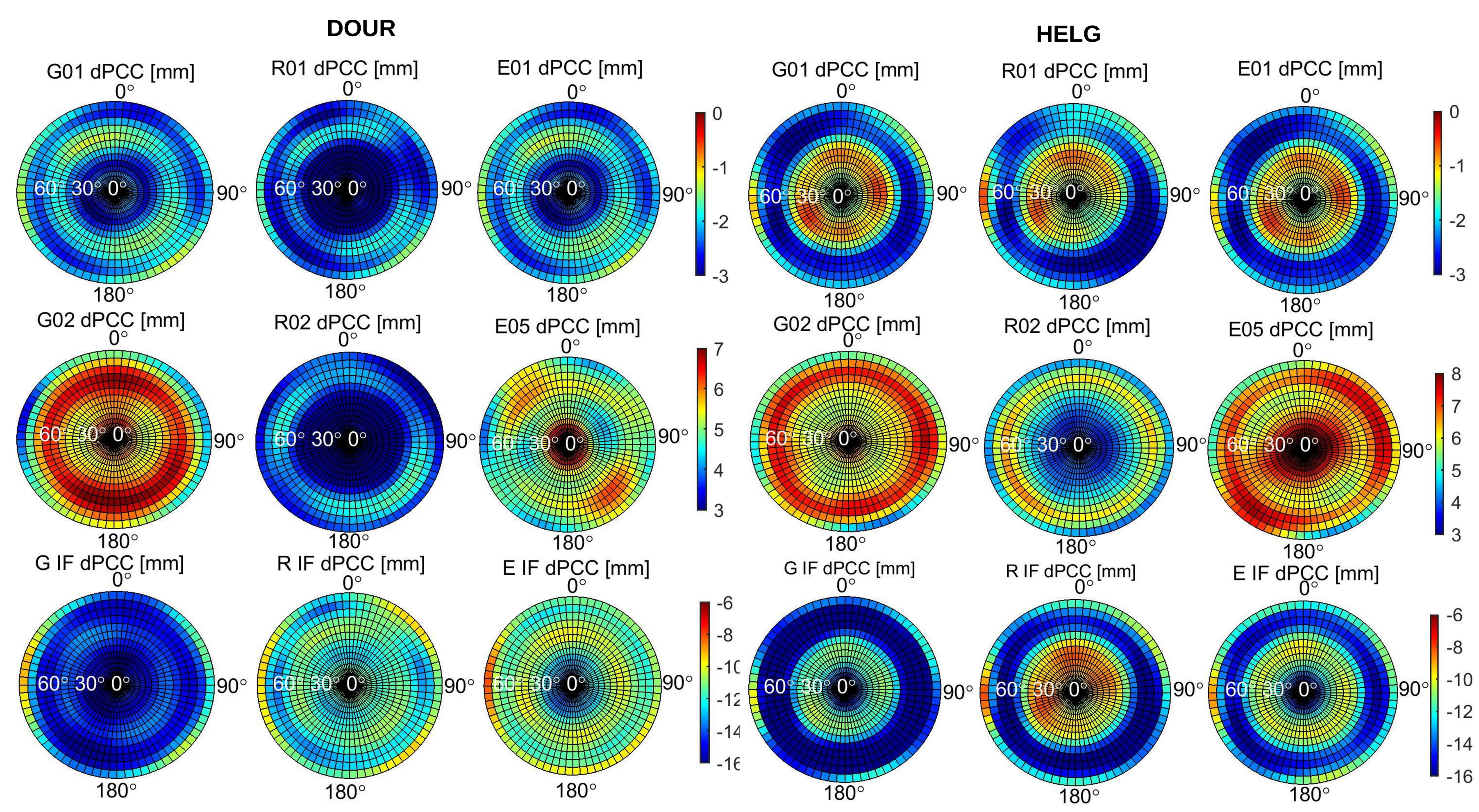

Fig 2. Azimuth and elevation dependent PCC differences obtained by comparison of chamber and robot calibration results for LEIAR25.R3 NONE antenna (stations DOUR and HELG).

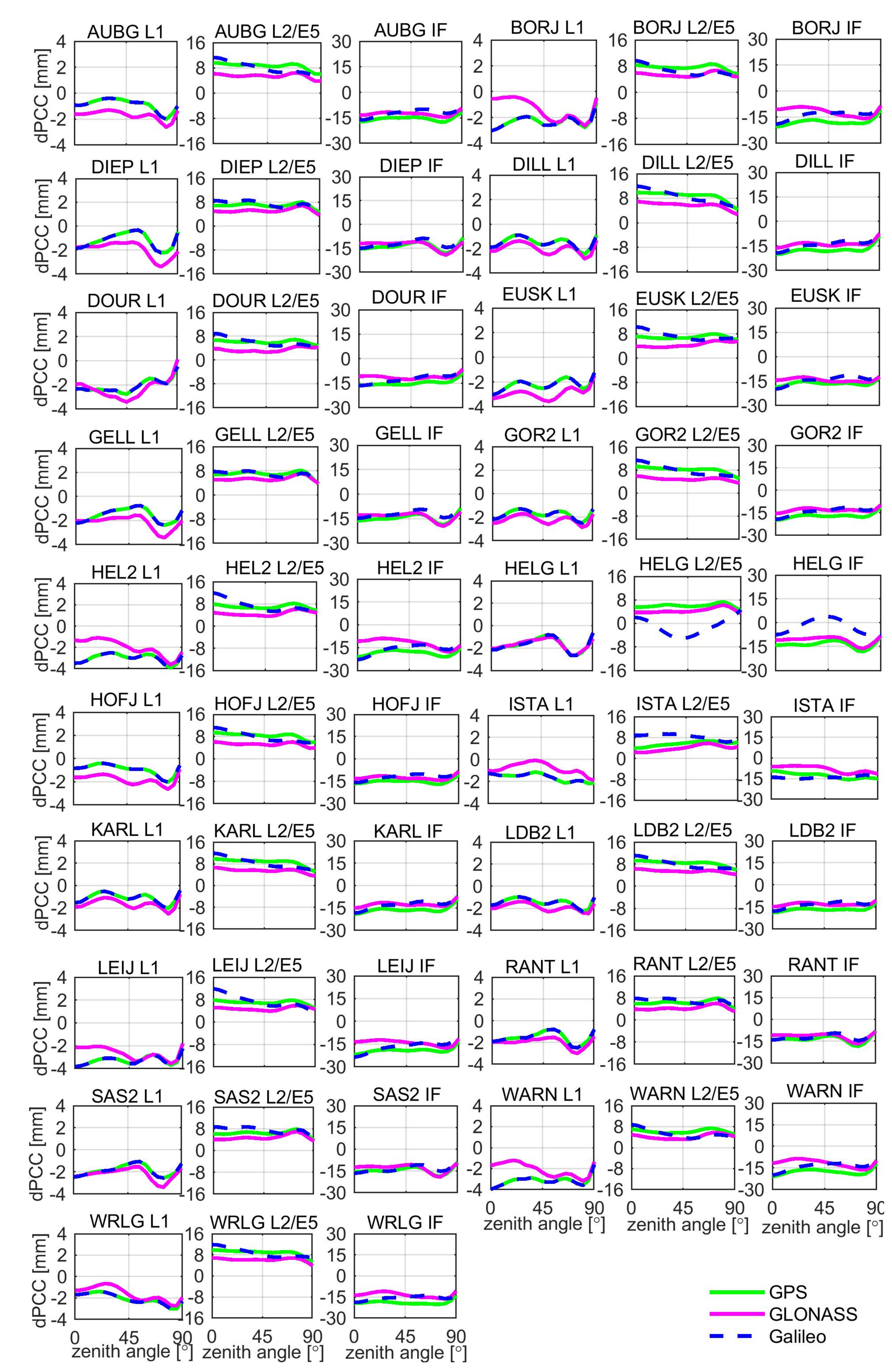

Fig 3. PCC differences obtained by comparison of chamber and robot calibration patterns as a function of zenith angle only.

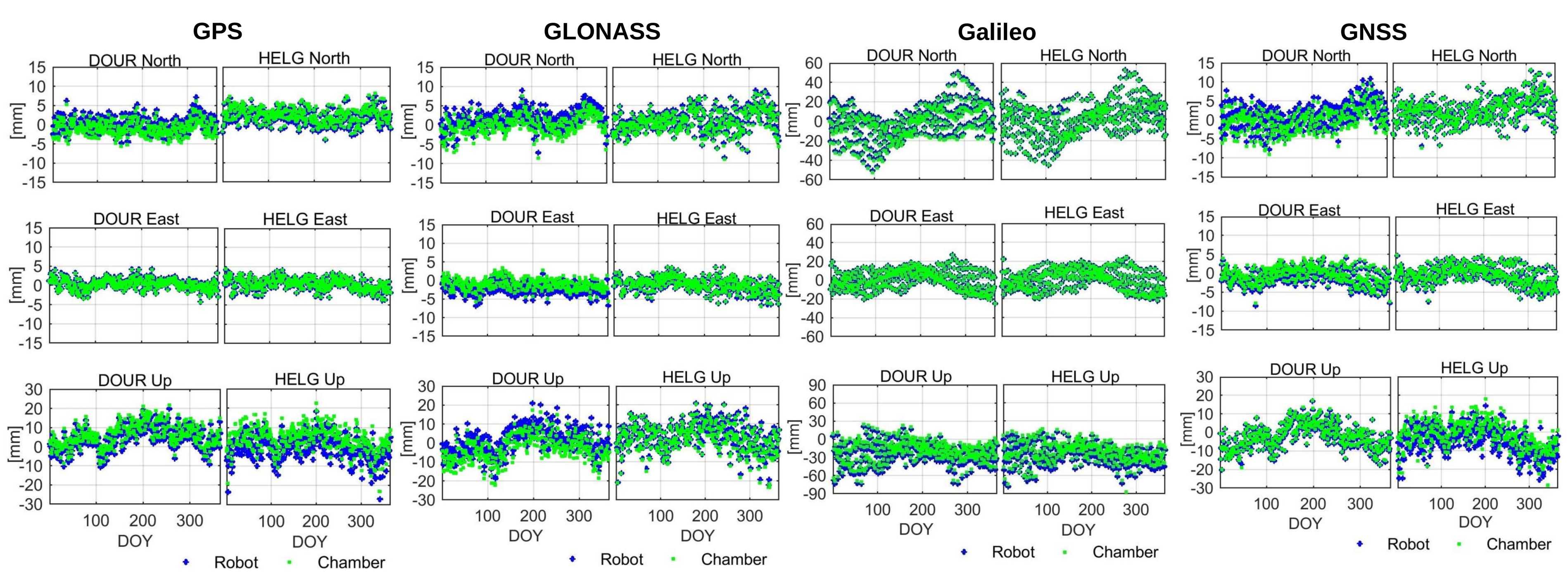

Fig 4. North, East, Up position component time series obtained in solutions with chamber and robot-derived PCC

Tab. 3. Mean position RMS obtained with robot and chamber-derived PCC models. ** stations with priority given to chamber model in EPN. * station ISTA is excluded from the average**

Station	RMS of position differences (ROBOT / CHAMBER) [mm]											
	GPS			GLONASS			Galileo			GNSS		
	North	East	Up	North	East	Up	North	East	Up	North	East	Up
AUBG	3.3 / 3.6	2.2 / 1.8	6.1 / 5.1	2.4 / 2.4	3.2 / 3.5	7.0 / 6.6	18.5 / 18.5	10.6 / 10.7	38.6 / 38.0	3.0 / 3.1	2.0 / 2.1	6.0 / 6.9
BORJ	2.2 / 2.3	2.2 / 2.0	6.2 / 6.5	3.0 / 2.8	2.3 / 2.2	7.7 / 11.9	17.8 / 18.0	10.8 / 10.8	**30.5 / 27.5**	3.5 / 3.5	2.9 / 2.9	8.7 / 11.2
DIEP	2.5 / 2.4	2.0 / 2.3	**5.6 / 9.6**	2.6 / 2.6	1.8 / 1.7	6.8 / 6.5	18.7 / 18.7	10.7 / 10.8	**35.7 / 26.9**	3.3 / 3.2	2.2 / 2.2	7.1 / 6.3
DILL	2.3 / 2.2	2.1 / 2.3	8.9 / 9.1	2.7 / 3.0	1.9 / 1.7	7.2 / 8.2	19.7 / 19.8	11.5 / 11.5	35.8 / 34.3	3.1 / 3.0	2.3 / 2.4	6.2 / 6.3
DOUR**	1.9 / 2.1	1.4 / 1.4	7.4 / 8.6	2.8 / 2.4	2.5 / 1.8	6.8 / 7.4	17.0 / 17.1	10.1 / 10.1	**29.6 / 25.9**	3.3 / 3.1	2.4 / 2.2	7.0 / 6.9
EUSK	2.6 / 2.7	2.7 / 2.9	8.1 / 8.1	2.6 / 2.8	1.7 / 1.8	7.3 / 9.0	19.2 / 19.1	11.2 / 11.5	34.6 / 31.8	3.2 / 3.3	2.5 / 2.6	6.8 / 7.3
GELL	2.4 / 2.6	2.8 / 2.1	**6.9 / 12.2**	2.5 / 2.7	1.7 / 1.8	6.4 / 6.6	19.6 / 19.4	10.9 / 10.8	**30.4 / 24.1**	3.2 / 3.5	2.4 / 2.2	6.7 / 7.4
GOR2	2.3 / 2.7	1.7 / 1.7	6.1 / 7.7	**2.3 / 3.5**	1.7 / 1.8	6.1 / 6.1	20.2 / 20.3	11.6 / 11.6	**32.1 / 28.3**	2.7 / 3.2	2.3 / 2.3	6.5 / 5.8
HEL2	3.3 / 4.2	1.7 / 2.5	6.8 / 8.3	2.7 / 2.5	**1.5 / 2.6**	6.9 / 7.4	18.9 / 19.0	11.0 / 11.2	**34.6 / 27.4**	3.6 / 3.9	2.2 / 2.8	7.4 / 7.1
HELG	2.8 / 3.2	1.5 / 1.6	6.3 / 7.5	3.0 / 3.0	2.2 / 2.1	7.9 / 7.7	17.7 / 17.6	10.4 / 10.4	**31.3 / 27.3**	4.2 / 4.3	2.4 / 2.4	8.9 / 7.6
HOFJ	2.4 / 2.4	4.4 / 3.9	6.2 / 6.7	2.6 / 2.5	2.6 / 2.4	7.6 / 7.4	19.3 / 19.4	11.1 / 11.2	35.3 / 34.2	2.8 / 2.8	2.3 / 2.3	7.7 / 9.0
ISTA**	62.8 / 63.0	37.5 / 37.6	**14.6 / 8.3**	62.2 / 62.7	40.3 / 40.0	**13.8 / 8.4**	64.9 / 64.9	38.7 / 38.7	36.9 / 38.7	63.1 / 63.5	38.8 / 38.7	10.4 / 8.1
KARL	2.4 / 3.2	3.0 / 3.2	6.4 / 6.5	3.3 / 4.2	2.4 / 2.6	8.1 / 8.0	17.6 / 17.7	10.6 / 10.6	29.3 / 27.2	3.6 / 4.0	3.5 / 3.7	8.3 / 8.2
LDB2	3.1 / 2.2	1.8 / 1.8	7.5 / 7.9	2.4 / 2.7	2.0 / 2.3	6.8 / 7.6	19.6 / 19.7	11.5 / 11.5	36.1 / 33.6	3.4 / 2.9	2.4 / 2.5	7.7 / 7.6
LEIJ	2.0 / 2.0	1.9 / 1.7	7.1 / 8.9	2.8 / 2.7	1.8 / 2.0	8.2 / 8.2	17.8 / 17.8	10.6 / 10.5	**29.2 / 23.2**	3.3 / 3.4	2.6 / 2.6	7.9 / 7.4
RANT	2.0 / 2.0	1.6 / 1.6	6.0 / 7.0	2.5 / 2.6	2.2 / 2.1	7.2 / 6.9	17.8 / 17.6	10.8 / 10.8	**31.6 / 27.7**	3.4 / 3.4	2.6 / 2.6	8.7 / 7.5
SAS2	2.2 / 2.3	1.9 / 1.9	7.0 / 9.7	3.0 / 2.9	2.7 / 2.8	9.1 / 8.8	18.1 / 18.1	10.8 / 10.8	**29.9 / 24.6**	3.8 / 3.8	2.9 / 2.9	8.5 / 7.8
WARN	2.1 / 1.9	1.9 / 1.9	5.9 / 6.3	2.6 / 2.4	2.0 / 2.0	**6.3 / 9.5**	18.0 / 18.0	10.9 / 10.8	**31.5 / 27.7**	3.3 / 3.4	2.7 / 2.7	8.3 / 8.7
WRLG**	2.5 / 2.8	2.3 / 1.9	**9.8 / 6.8**	2.3 / 2.5	1.9 / 1.8	8.2 / 9.0	18.1 / 18.1	11.5 / 11.6	32.4 / 33.6	3.1 / 3.3	2.7 / 2.5	6.6 / 8.0
average RMS***	**2.5 / 2.6**	**2.1 / 2.1**	**6.9 / 7.9**	**2.7 / 2.8**	**2.1 / 2.2**	**7.3 / 7.9**	**18.7 / 18.6**	**10.9 / 11.0**	**32.7 / 28.5**	**3.3 / 3.4**	**2.5 / 2.6**	**7.5 / 7.6**

Results and summary

Comparison of PCC models obtained from the absolute field calibration and the calibration in the anechoic chamber revealed differences of up to 20 mm in the case of the IF combination. For L1 and L2 frequencies these differences were visibly smaller, but their maximum values were close to 5 mm for L1 and exceeded 10 mm for L2 signals. These differences should be considered significant, if millimeter accuracy of the position components is expected.

In analyzing the results obtained for the 24-hour solution time series based on GPS, GLONASS and GNSS solutions, for the North component the differences between the obtained and reference coordinates were below ±10 mm, for the East component they do not exceeded ± 5 mm, and for the vertical component they reached up to ± 20 mm. However for Galileo the discrepancies were much higher reaching up to 40 mm, 20 mm and 50 mm for Northing, Easting and Up, respectively.

The differences of coordinates, obtained from averaging daily results from robot and chamber calibration solutions, rarely exceeded ± 2 mm in horizontal components and ± 10 mm in heights. Average deviations for GPS, GLONASS, Galileo and GNSS solutions proved very similar, being close to 0.6 mm, 0.5 mm and 4.8 mm for Northing, Easting and Up, respectively.

Comparing the results from both types of calibrations with the reference coordinates from the cumulative EPN solution, a noticeable advantage of one of the solutions occurred primarily in the case of height determinations. For stations ISTA and WRLG with priority given to chamber calibration in EPN the advantage in height determination RMS of solution utilizing this calibration ranged from 3 to 5 mm. The advantage of chamber calibration occurred also at most stations in the Galileo solution, where height RMS difference exceeded even 8 mm. In the set of stations with priority given to robot calibration the significant predominance of this type of calibration, exceeding 3 mm RMS difference occurred at 3 stations (DIEP, GELL, BORJ) in the GPS and GLONASS solution. For horizontal coordinates, however, only station HEL2 revealed the noticeable advantage of any solution, exceeding the threshold of 1 mm in favor of the solution utilizing the calibration from the robot in the GLONASS solution. For other stations the differences between solutions can be considered as insignificant.